Journal of Geophysical Research: Biogeosciences

RESEARCH ARTICLE
10.1029/2018JG004416

Making Sense of Massive Carbon Isotope Excursions With an Inverse Carbon Cycle Model

Yoshinori Miyazaki[1], Noah J. Planavsky[1], Edward W. Bolton[1], and Christopher T. Reinhard[2]

[1]Department of Geology and Geophysics, Yale University, New Haven, CT, USA, [2]School of Earth and Atmospheric Sciences, Georgia Institute of Technology, Atlanta, GA, USA

Key Points:
- Large positive or negative excursions in marine $\delta^{13}C_{DIC}$ values are modeled with plausible redox fluxes
- Sedimentary recycling and an oxygen dependence on organic carbon oxidation are introduced in our global carbon cycle models
- Our model dramatically reduces the magnitude of redox imbalance required to explain large $\delta^{13}C$ excursions

Supporting Information:
- Supporting Information S1

Correspondence to:
Y. Miyazaki and N. J. Planavsky,
yoshinori.miyazaki@yale.edu;
noah.planavsky@yale.edu

Citation:
Miyazaki, Y., Planavsky, N. J., Bolton, E. W., & Reinhard, C. T. (2018). Making sense of massive carbon isotope excursions with an inverse carbon cycle model. *Journal Geophysical Research: Biogeosciences*, *123*, 2485–2496. https://doi.org/10.1029/2018JG004416

Received 24 JAN 2018
Accepted 20 JUN 2018
Accepted article online 26 JUN 2018
Published online 22 AUG 2018

Abstract The beginning and end of the Proterozoic Eon are marked by extreme variations in carbonate carbon isotope values that have been interpreted to record massive perturbations to the global carbon cycle. The lower Proterozoic contains an extended interval of strata characterized by positive carbonate $\delta^{13}C$ values. Conversely, uppermost Proterozoic carbonate strata contain thick intervals with extremely negative $\delta^{13}C$ values and multiple large swings in carbonate $\delta^{13}C$. Previous attempts to model these pronounced carbon isotope excursions as shifts in the global marine dissolved inorganic carbon (DIC) reservoir have proved to be problematic, as the direction and magnitude of these positive and negative carbon isotope excursions require unrealistic amounts of either organic carbon burial or organic carbon oxidation, respectively. Here we present a modified global carbon cycle model—coupled with oxygen and sulfur cycle mass balances—that includes a parameterization of the recycling of sedimentary isotope anomalies and allows the extent of organic carbon oxidation to vary as a function of atmospheric oxygen levels. Our model is designed to match carbon isotope records while maintaining redox and mass balance with a given set of initial conditions and carbon cycle parameterizations. Using this approach, we demonstrate that there is a range of plausible biogeochemical perturbations that could induce substantial $\delta^{13}C$ excursions in the global marine DIC reservoir. However, we also find that there are multiple, nonunique Earth system states for any observed marine $\delta^{13}C$ value.

1. Introduction

The Proterozoic Eon (~2.5 to 0.5 billion years ago, Ga), was bookended by extreme perturbations to global biogeochemical cycles with intervening periods of apparent stability. This trend is reflected foremost in the carbonate carbon isotope record ($\delta^{13}C_{carb}$; Krissansen-Totton et al., 2015; Shields & Veizer, 2002). The Proterozoic contains an extended period of markedly positive carbonate carbon isotope values referred to as the Lomagundi carbon isotope excursion. The Lomagundi has a near-global distribution and has been commonly linked to increased organic carbon burial (e.g., Bekker et al., 2014). However, using a traditional carbon isotope mass balance, the amount of oxygen from organic carbon burial produced from this excursion is extreme—over 10 to 20 times the modern atmospheric reservoir (Karhu & Holland, 1996). It is true that numerous lines of evidence suggest this interval is marked by an increase in atmospheric oxygen levels relative to the low levels that characterized the Earth's early history (Blättler et al., 2018; Kump et al., 2011; Partin et al., 2013; Planavsky et al., 2012; Yokota et al., 2013), but many of the obvious signatures of a well-oxygenated (Phanerozoic like) ocean-atmosphere system are absent from the Paleoproterozoic sedimentary record (Lyons et al., 2014). Kump and others have also proposed that there was a pronounced negative isotope anomaly after the Lomagundi excursion, linked to atmospheric oxygen rise and the long-term accumulation of organic matter in the upper continental crust during the excursion (Kump et al., 2011).

The mid-Proterozoic (~1.8–0.8Ga) is marked by carbon isotope stability, which has led to this interval being referred to as the "Boring Billon" (Lindsay & Brasier, 2002). This inferred carbon cycle stability has been linked to strong nutrient limitation, redox stability, and a large DIC reservoir (Bartley & Kah, 2004; Derry, 2015; Reinhard et al., 2017). Further, although numerous eukaryotic clades evolved during the mid-Proterozoic, this interval is marked overall by low rates of speciation, low eukaryote abundance, and limited eukaryotic morphological disparity (Brocks et al., 2017; Knoll, 2015). The exact levels of atmospheric oxygen present in the mid-Proterozoic are debated (e.g., Liu et al., 2016; Planavsky et al., 2014; Yokota et al., 2013; Zhang et al., 2016),

but there is support for an increase in surface oxygen levels later during the Neoproterozoic (Kump, 2008; Lyons et al., 2014; Shields-Zhou & Och, 2011).

Around 800 million years ago (Ma) there is evidence for a marked increase in carbon isotope variability, the onset of Neoproterozoic oxygenation, and a marked increase in biological innovation (Cole et al., 2016; Halverson et al., 2005; Planavsky et al., 2015; Thomson et al., 2015; Turner & Bekker, 2016). Numerous workers have proposed that these shifts record the onset of a more dynamic global carbon cycle (e.g., Bjerrum & Canfield, 2011). Prominent carbon isotope excursions are found throughout the Neoproterozoic. The largest carbon excursion is the so-called Shuram-Wonoka or Shuram excursion that is thought to have occurred at roughly 580 Ma. The Shuram excursion was initially found in the Huqf Supergroup of Oman (Burns & Matter, 1993), and there has been subsequently identified in South China (McFadden et al., 2008), Australia (Calver, 2000), and Sibera (Pokrovsky & Gertsev, 1993), among other localities. The isotopic composition of carbonate in sedimentary rocks during this anomaly drops to as low as −12‰—well below the canonical mantle value of −5.5‰ (Fike et al., 2006). These low values are inexplicable using a traditional view of the global carbon cycle (e.g., Kump & Arthur, 1999), as values below the mantle input value on million-year time scales require both an almost complete cessation of marine primary production and a large unidentified source of ^{12}C-enriched carbon (cf. Holland, 1984).

It has been argued that a long-lived (i.e., several million years) markedly negative carbon isotope excursion is very difficult to obtain without violating redox or mass balance (Bristow & Kennedy, 2008; Shi et al., 2017). Although this anomaly has arguably been found globally, there is still ongoing debate about whether the extreme negative carbon isotope values have a primary or a diagenetic origin (e.g., Derry, 2010; Oehlert & Swart, 2014). Foremost, the negative $\delta^{13}C_{carb}$ values could be linked to overprinting from basinal brines (Derry, 2010) or meteoric fluids (Knauth & Kennedy, 2009). Further work constraining the effects of diagenesis on the end Proterozoic carbonate record is thus critical. Nevertheless, we feel that there is still strong impetus to develop a new quantitative framework for exploring the factors that can drive markedly negative global marine carbon isotope excursions.

Numerous mechanisms have been proposed to explain a Shuram-like global marine DIC isotope excursion. However, most mechanisms are, by necessity, at their core nonsteady state carbon cycle models in which there is extensive organic matter oxidation. Marine dissolved organic carbon (e.g., Fike et al., 2006; Rothman et al., 2003), petroleum (Lee et al., 2013), and terrestrial organic matter have all been invoked as the organic material being oxidized (Shi et al., 2017). Regardless of the carbon source, a significant concern for all primary Shuram models is whether there are sufficient oxidants to drive the isotopic composition of global marine DIC to values markedly below the mantle input. Further, quantitative models have not yet produced a global carbon cycle that can reproduce the Shuram excursion if the carbonate records were tracking the marine DIC reservoir and the duration of the excursion was millions of years (Bristow et al., 2012; Shi et al., 2017). If the duration of the anomaly was short lived (<1 Myrs), oxidation of methane could potentially drive the excursion (Bjerrum & Canfield, 2011). However, this is at odds with geologic constrains on the excursion time scale (e.g., Gong et al., 2017; Le Guerroue et al., 2006), and this model requires an extremely large pulsed methane flux (100 times modern) without an obvious trigger.

Here we present a global carbon cycle model that can produce pronounced negative carbon isotope excursions on million-year time scales with plausible redox fluxes. Similarly, the model can produce large positive carbon isotope excursions without transitioning to extremely high pO_2 levels or invoking abnormally high reductant fluxes. In contrast to previous carbon cycle models that have been used to explore the Proterozoic carbon isotope record (e.g., Bristow & Kennedy, 2008), we allow the extent of carbon oxidation to vary with atmospheric oxygen levels (cf. Bolton et al., 2006, Derry, 2015) and we include recycling of sedimentary rock masses from the marine to the terrestrial realm (following Berner, 1987 and Reinhard et al., 2013). Further, similar to approaches that have been used to explore the Cenozoic carbon isotope record (e.g., Ridgwell & Schmidt, 2010), our model is designed to match a real or idealized carbon isotope record with a minimum number of prescribed forcings. Redox balance is maintained by the sulfur cycle, while oxygen mass balance and carbon isotope mass balance are forced. With this approach, we cannot propose a unique solution for any given carbon isotope excursion. However, we can demonstrate that extreme global marine carbon isotope excursions are possible in an Earth system in which the carbon isotope composition of the input term can vary substantially as a function of atmospheric O_2. In other words, extreme global marine carbon isotope excursions are possible if there are large swings in atmospheric O_2 levels.

2. Method

Our model is based on a commonly utilized long-term carbon isotope mass balance (Kump & Arthur, 1999). The surface carbon cycle is governed by inputs to the system (weathering of continents, metamorphism, and volcanism) and outputs (carbonate and organic sediment burial). In turn, these fluxes and their isotope compositions play an important role in determining the isotope value of marine DIC (δ_{carb}). Two key properties regulating this evolution are the following: (1) the isotopic composition of the integrated inputs into the ocean-atmosphere system (δ'_w) and (2) the relative fraction of organic burial relative to total outputs. Conventional long-term models have treated the isotopic composition of the input flux as a constant value, mimicking the mantle input (cf. Holland, 1984). However, the $\delta^{13}C$ value of the globally integrated input flux should have also changed dynamically with shifts in surface oxygen levels (e.g., Daines et al., 2017; Derry, 2015; Holland, 2002). Building on this idea, our model allows for input of carbon to the ocean-atmosphere system derived from organic carbon oxidation to vary with pO_2. Specifically, following Derry (2015) and building from the work of Bolton et al. (2006), we used a terrestrial organic carbon oxidation model to estimate global organic carbon oxidation efficiencies. The model assumes that black shale is the primary host of organic carbon, and atmospherically derived gaseous O_2 diffuses through interconnected pore spaces to oxidize available organic carbon. We used probability density functions to account for the fact that local erosion rates and local *bedrock* organic carbon concentrations will vary, and we include oxidation during both soil formation and overbank storage/transport (supporting information Figure S3). A similar approach was recently utilized and described in detail by Daines et al. (2017). Further, following previous parameterizations of the rock cycle (Berner, 1987; Reinhard et al., 2013), we allow the isotopic composition of the weatherable shell (i.e., the rocks at Earth's surface being subjected to weathering) to vary through the excursion via sedimentary rock recycling. Lastly, in a subset of runs, we model the release of potentially light CO_2 from carbonatites, recently suggested as a possible driver of the Shuram excursion (Paulsen et al., 2017). In these cases, in addition to the usual volcanic flux, we add an 0–2 Tmol/year of a carbonatite CO_2 flux with $\delta^{13}C$ value of −10‰.

The amount of carbon in the ocean and atmosphere, M_0, is assumed to be constant, and its isotopic composition ($\delta^{13}C_{carb}$) changes with the isotopic composition of carbon inputs (δ'_w as above) and the outputs (organic carbon and carbonate burial), as well as the isotopic offset between organic and inorganic carbon (Δ_B):

$$M_0 \frac{d\delta_{carb}}{dt} = F_w(\delta'_w - \delta_{carb}) - F_{b,org}\Delta_B \tag{1}$$

where F_w and $F_{b,org}$ denote the flux magnitude of total input to the ocean-atmosphere system and organic carbon burial, respectively. Input to the surface is composed of four components: volcanic, methane release, carbonate weathering, and organic weathering:

$$\delta'_w = \frac{F_{volc}\delta_{volc} + F_{CH_4}\delta_{CH_4} + F_{w,carb}\delta_{w,carb} + F_{w,org}\delta_{w,org}}{F_{volc} + F_{CH_4} + F_{w,carb} + F_{w,org}}, \tag{2}$$

where F_{volc}, F_{CH_4}, $F_{w,carb}$, and $F_{w,org}$ refer to the flux of carbon from volcanic and methane sources, carbonate weathering, and organic weathering, respectively, and δ_i terms refer to their respective isotopic compositions.

Following Berner (1987), the weathering inputs of carbon in our model are sourced from two crustal reservoirs (young and old) with different recycling rates of sedimentary organic and carbonate carbon. This model parametrization was originally invoked based on evidence that a portion of newly deposited sediments are rapidly introduced into the weatherable shell (Berner, 1987). The mass of both young (rapid weathering; $M_{carb,y}$) and old (slow weathering; $M_{carb,o}$) reservoirs are set to be constant throughout the evolution, and their isotope compositions are given by

$$\frac{d\delta_{carb,y}}{dt} = \frac{F^{b,carb}_{surf\to y}(\delta_{carb} - \delta_{carb,y})}{M_{carb,y}} \tag{3}$$

$$\frac{d\delta_{carb,o}}{dt} = \frac{F_{y\to o}(\delta_{carb,y} - \delta_{carb,o})}{M_{carb,o}} \tag{4}$$

where $\delta_{carb,y}$ and $\delta_{carb,o}$ denote the isotopic composition of young and old crustal carbonate reservoir, respectively. The fluxes $F^{b,carb}_{surf\to y}$ and $F_{y\to o}$ respectively show the flux size of carbonate burial added to the young crust and the gradual transport of the young to the old crust. The carbonate weathering comes from both young and old reservoirs, the isotopic composition of which is described as follows:

$$\delta_{w,carb} = \frac{F_{carb,y\rightarrow surf}\delta_{carb,y} + F_{carb,o\rightarrow surf}F_{carb,o\rightarrow surf}}{F_{carb,y\rightarrow surf} + F_{carb,o\rightarrow surf}} \quad (5)$$

where $F_{carb,y\rightarrow surf}$ and $F_{carb,o\rightarrow surf}$ show the flux magnitudes of weathering from young and old crustal reservoir, respectively. These fluxes are balanced to maintain the size of each reservoir. We implement the same formulations for organic carbon in the crustal reservoir. Two organic carbon reservoirs, young (rapid weathering; $M_{org,y}$) and old (slow weathering; $M_{org,o}$), are introduced to the model. The total magnitude of organic carbon being weathered is a function of pO_2, following the approach of Bolton et al. (2006) and Derry (2015) (supporting information Figures S1–S3).

For the early Proterozoic (Lomagundi) runs, we have assumed a Δ_B value of −30‰, generally consistent with compiled averages (e.g., Krissansen-Totton et al., 2015). For the late Proterozoic (Shuram) runs, we have assumed that the newly buried organic carbon has a Δ_B value of −25‰, whereas the isotopic composition of initial organic carbon in the crustal reservoir is set to −30‰. This corresponds to a Δ_B value of −30‰ reflecting the evolution of organic materials in the Proterozoic. There are numerous factors that shape the fractionation between organic and inorganic carbon (Δ_B values), including pCO_2, growth rates, and remineralization pathways (e.g., Hayes et al., 1999; Kump & Arthur, 1999), and we have not explicitly modeled this fractionation. However, it is not unreasonable (e.g., outside of error in current records; Krissansen-Totton et al., 2015) to suggest that long-term average fractionation decreased toward the end of the Proterozoic. Additionally, mid-Proterozoic rocks are in general more thermally mature than end-Proterozoic rocks, making it difficult to precisely contain the temporal evolution of Δ_B values from empirical records.

The evolution of atmospheric oxygen levels is driven by organic carbon burial and oxidation based on a commonly utilized idealized organic stoichiometry (an assumed $CH_2O + O_2 \rightarrow CO_2 + H_2O$ reaction). Overall atmospheric oxygen levels are set by the balance between organic burial rate ($f_{org} = F_{b,org}/F_w$) and oxidative weathering. The evolution of the atmospheric oxygen reservoir is described as (Berner, 1987)

$$\frac{dM_{O_2}}{dt} = F_{b,org} + \frac{15}{8}F_{b,py} - F_{w,org} - F_{MORB}, \quad (6)$$

where $F_{b,py}$ denotes the burial flux of pyrite sulfur and F_{MORB} shows oxygen consumption at mid-ocean ridges, which is set to 1 Tmol/year for $pO_2 > 40\%$ PAL (Derry, 2015; Lécuyer & Ricard, 1999), while 0.1 Tmol/year is adopted in an anoxic condition. This number is based on common estimates for the atmospheric pO_2 values requires to oxygenate the deep ocean (e.g., Canfield, 1998; Kump, 2008). However, we acknowledge that this cutoff is somewhat arbitrary, as there are very poor constraints on the strength of the biological pump in the Precambrian and this almost certainly varied dramatically through time. In any case, oxidant shortage is the major barrier for reproducing the Shuram excursion, indicating that in general a higher threshold would make Shuram-type excursions easier to reproduce (discussed below).

Atmospheric oxygen levels directly affect the sulfur cycle. However, the exact mechanistic links between the sulfur and oxygen cycles is not well constrained even for the Cenozoic. Further, the sulfur cycle is also strongly influenced by tectonic factors (Halevy et al., 2012; Wortmann & Paytan, 2012). For the Shuram model we specified that there was an imbalance between weathering and burial of pyrite (i.e., there was a net transfer of oxidants from the crust to the ocean-atmosphere system). In the preferred model runs we allowed a maximum imbalance of 1 Tmol/year between reduced and oxidized sulfur, converting sedimentary sulfate to pyrite, which is roughly one third of the current total sulfur input to the marine system (e.g., Berner & Berner, 2012). This number is consistent with estimates of the extent of variations in the ratio of pyrite to total sulfur burial (f_{py}) observed through the Neoproterozoic and Phanerozoic (e.g., Canfield & Farquhar, 2009; Halevy et al., 2012; Wu et al., 2010).

The size of the reservoirs and fluxes is summarized in Figure 1 and is also listed in Appendix A. As noted above, the oxygen level determines the size and the isotope composition of the weathering flux. For Shuram runs, we impose a net forcing from the S cycle and then evaluate the f_{org} value required to match a given marine $\delta^{13}C_{DIC}$ value. When modeling the Lomagundi excursion, the goal is to prevent a massive release of oxygen and carbon dioxide drawdown. Therefore, we use the same modeling method as the Shuram runs, including the rapid cycling of carbonate sediments and the suppression of organic carbon weathering under a low oxygen atmosphere, but instead of imposing a sulfur burial flux, we fix atmospheric oxygen levels and investigate the net pyrite consumption necessary to maintain a given level of oxygen.

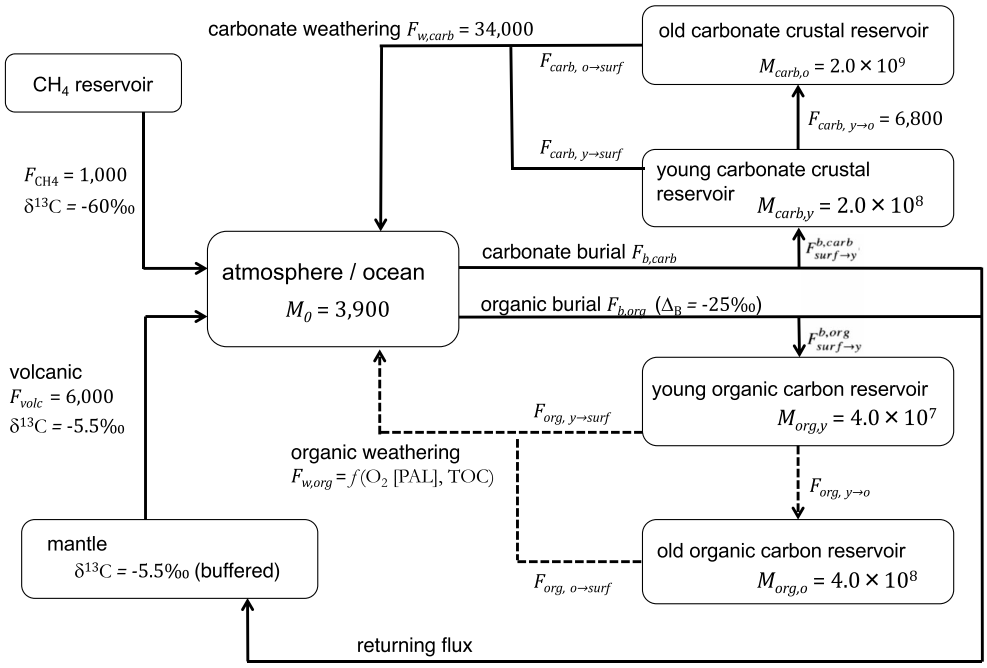

Figure 1. Schematic diagram of our model structure showing the reservoirs and fluxes given in equations (1)–(5). Fluxes are in units of 10^{12} mol C/kyr, and reservoirs are in units of 10^{12} mol C. Solid lines refer to a constant fluxes, whereas dotted lines denote organic carbon weathering fluxes that vary as a function of atmospheric pO_2 and total organic carbon content.

3. Results

3.1. Shuram Excursion

Our model can reproduce the Shuram excursion with an excursion duration between 10 and 30 Myr without introducing large amounts of methane into the ocean-atmosphere system and with only modest changes to the crustal sulfur redox balance (Figures 2 and 3). Here we assume that the carbonate carbon isotope results from Fike et al. (2006) track the global marine DIC reservoir. Although model outputs vary depending on the duration of the excursion and the amount of organic carbon in the weatherable shell (supporting information Figure S3), all model runs follow a similar evolutionary sequence. The model predicts a short-lived increase in oxygen during the initial stage of the Shuram excursion coincident with an increase in the weathering of organic carbon. The initial increase in atmospheric oxygen levels is driven in part by increased pyrite burial. Extensive organic carbon oxidation releases light carbon ($\delta^{13}C = -30‰$) to the ocean-atmosphere system and consumes oxygen, thereby decreasing pO_2 levels. This in turn lowers the amount of organic matter being oxidized. Atmospheric oxygen levels remain low relative to the initial condition throughout the duration of the carbon isotope excursion, before increasing when $\delta^{13}C_{carb}$ values returns to positive values. The extent of the shift in atmospheric oxygen levels becomes more severe the longer the duration of the carbon isotope excursion. In addition to this biogeochemically forced change in seawater $\delta^{13}C_{DIC}$, light sedimentary carbon deposited during the excursion is recycling back into the weatherable shell, helping to maintain a long-term shift in the $\delta^{13}C$ value of the integrated input term. When such rapid recycling of light carbon is not included, the model causes an *oxidant crisis*. The lack of recycling results in a heavier value for the weathering, which requires more extensive weathering of light organic carbon to drive the excursion and thus consumes larger amount of atmospheric oxygen (Figure 2).

We have also explored the effect of a light (−10‰) CO_2 *carbonatite flux* between 0 and 2 Tmol/year, given a recent suggestion that this process could be the main driver of the Shuram carbon isotope excursion (Paulsen et al., 2017). Carbonatites would be a major component of total outgassing flux with the maximum flux (between 10% and 20% of the modern flux; Wallmann & Aloisi, 2012). Critically, in all of these cases the carbonatite flux results in a minor shift in the biogeochemical parameters needed to force the carbon isotope excursion. Carbonatite CO_2 fluxes, with lighter carbon than the typical volcanic input, result in less organic matter oxidation being needed to drive the marine DIC reservoir to strongly negative values. However, rela-

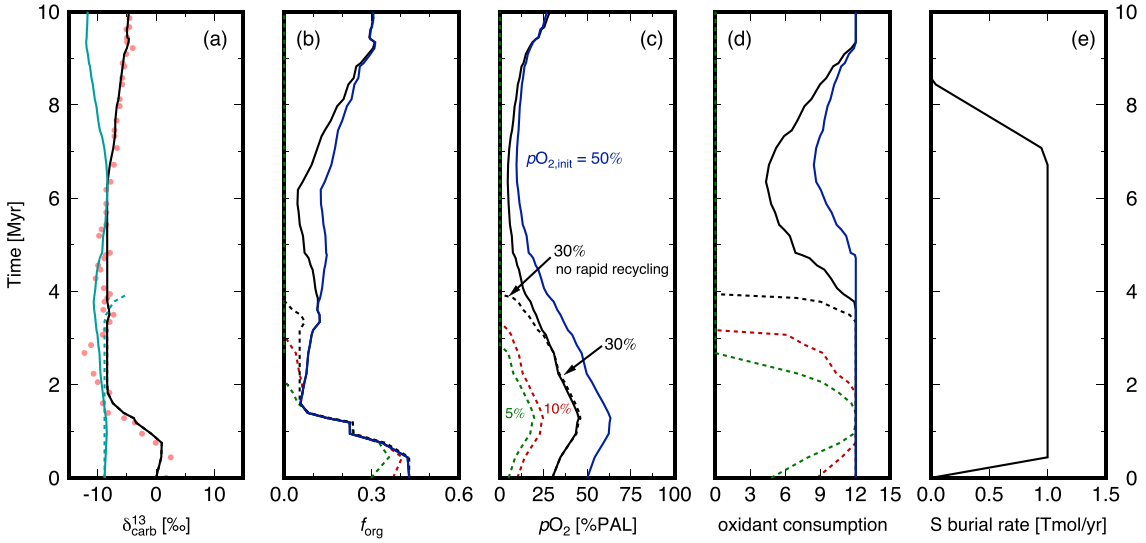

Figure 2. (a) Modeled isotopic values of marine DIC during the Shuram excursion (solid black) for a 10-Myr duration and an initial atmospheric oxygen level of 30% the present atmospheric level (PAL). Carbonate $\delta^{13}C$ data from Fike et al. (2006) are shown as filled circles. The $\delta^{13}C$ value of the weathering flux is also shown for a model with (solid cyan) and without (dashed cyan) rapid recycling. (b–e) Model results for runs with initial pO_2 values of 5% (dashed green), 10% (dashed red), 30% (solid black), and 50% PAL (solid blue) are shown. The dashed lines indicate failed runs where negative f_{org} or pO_2 is necessary to satisfy mass balance. (b) Relative organic carbon burial fraction (f_{org}). (c) Atmospheric oxygen level. (d) Rate of oxidant consumption (e.g., net weathering rate of organic carbon). (e) Required net imbalance between the weathering and burial of pyrite. The figure is shown as the mole of sulfur atom, rather than the mole of pyrite.

tive to the noncarbonatite model runs there will be higher oxidant consumption because of higher oxygen levels, resulting in similar overall biogeochemical fluxes. Further, the effect of even the largest carbonatite CO_2 fluxes only changes the extent of oxidant consumption by ~10%, a much smaller effect than either rapid recycling or oxygen dependent organic carbon weathering (supporting information Figure S9).

By design, our model can reproduce marine $\delta^{13}C_{DIC}$ values that match Shuram carbon isotope records under a wide range of possible carbon cycle perturbations. However, it is important to consider if certain boundary conditions and model features yield physically unrealistic carbon cycle parameters. Specifically, for multimil-

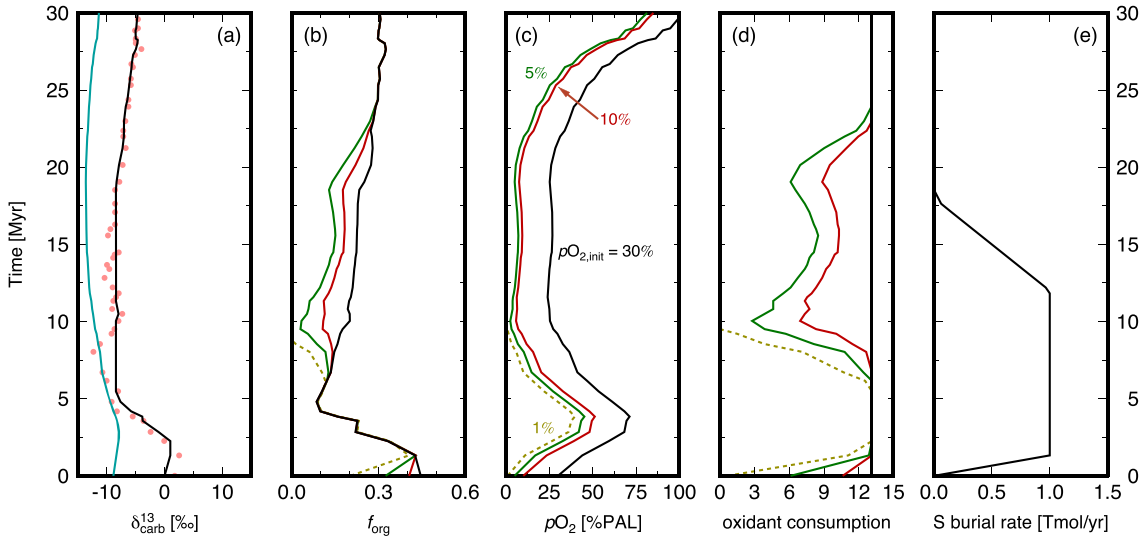

Figure 3. (a) Modeled isotopic values of marine DIC during the Shuram excursion (solid black) for a 30-Myr duration and an initial atmospheric oxygen level of 30% the present atmospheric level (PAL). Carbonate $\delta^{13}C$ data from Fike et al. (2006) are shown as filled circles. The $\delta^{13}C$ value of the weathering flux is also shown (solid cyan). (b–e) Model results for runs with initial pO_2 values of 1% (dashed yellow) 5% (solid green), 10% (solid red), and 30% PAL (solid black) are shown. The dashed lines indicate failed runs where negative f_{org} or pO_2 is necessary to satisfy mass balance. (b) Relative organic carbon burial fraction (f_{org}). (c) Atmospheric oxygen level. (d) Rate of oxidant consumption (e.g., net weathering rate of organic carbon). (e) Required net imbalance between the weathering and burial of pyrite. The figure is shown as the mole of sulfur atom, rather than the mole of pyrite.

lion year excursions, initial pO_2 levels lower than 10% PAL result in either shortage of atmospheric oxygen or exceptionally low f_{org} values (<0.1) during the initial carbon isotope nadir. At the highest pO_2 levels explored here the amount of organic carbon being weathered increases above 10 Tmol/year, which may not be sustainable when integrated over millions of years (e.g., Derry, 2015). There are poor constraints on surface oxygen levels in the Proterozoic (Lyons et al., 2014). However, in our model an initial pO_2 level of 10–30%PAL, depending on the duration, best explains the excursion. This is consistent with a pO_2 level over 5%PAL during the late Neoproterozoic, suggested by recent oxidation modeling work (Yokota et al., 2013) and still consistent with the presence of largely anoxic ocean (Sperling et al., 2015). Lastly, our model only functions when there is net conversion of sedimentary sulfate into sedimentary pyrite, which compensates for an extensive consumption of atmospheric oxygen during organic carbon weathering. However, given that there are massive evaporites deposited in Tonian basins (Turner & Bekker, 2016) this is likely not an unreasonable flux to invoke. The shortage of oxidant (atmospheric oxygen) is the major barrier for reproducing the Shuram excursion, indicating that higher threshold for MORB oxidation provides an easier condition to reproduce the excursion. When the threshold for MORB oxidation is set to be lower, however, more atmospheric oxygen will be consumed, causing a failure to simulate the excursion (supporting information Figure S12).

3.2. Lomagundi Excursion

We present model runs of an idealized Lomagundi carbon isotope excursion at four different pO_2 levels (1%, 10%, 30%, and 50% PAL). The duration and structure of the Lomagundi carbon isotope excursion are still being developed (Bekker, 2014); and therefore, we have chosen to simply explore the signature of a large, long-lived positive isotope excursion with a Gaussian perturbation. This is, of course, a simplification of the actual structure of the excursion (e.g., Bekker & Holland, 2012) but should produce reasonable overall behavior within the biogeochemical model.

Using a standard carbon cycle model and keeping pO_2 fixed at a given level, the redox imbalance tied to the sulfur cycle is greater than 3 Tmol/year in most model runs (Figure 4). This is larger than the entire modern sulfur input flux and represents an unlikely Earth system state as it implies all sulfur is being weathered as pyrite and buried as sulfate. However, including sediment recycling and oxygen dependence on organic carbon oxidation dramatically decreases the oxidant release of the excursion. As seen in all runs with rapid recycling of carbonate sediments, the isotopic value of the young crustal reservoir rises quickly, whereas the old reservoir experiences a minor increase of ~1‰. The carbonate weathering flux does not change between any of the runs, but the degree of organic carbon weathering increases with higher oxygen level, driving the isotopic value of an integrated inputs to a lighter value. These two effects combined create a heavier input and result in carbon burial rates that are dramatically lower than previous model estimates (Figure 4; Bachan & Kump, 2015; Karhu & Holland, 1996). With these modifications, the redox imbalance tied to the sulfur cycle remains below 1.5 Tmol/year in most model runs, which is roughly half of the modern sulfur input flux. Note that 30% PAL and 50% PAL runs show only a small difference in carbon burial rate because the oxidation power of organic carbon largely saturates above 20% PAL, which may not be fully accurate (see Derry, 2015), but for our purposes here is conservative.

4. Discussion

4.1. Shuram Excursion

One of the principle motivations for this work was that previous attempts to model the Shuram carbon isotope excursion have concluded that there was a shortage of the oxidants needed to drive the global marine DIC reservoir to markedly light carbon isotope values—especially for an excursion lasting millions of years (see Bristow & Kennedy, 2008). Our inverse approach alleviates this *oxidant paradox*: the combination of inhibited organic carbon oxidation at lower atmospheric oxygen levels and recycling of light organic matter from recently deposited sediments back into the weatherable shell (Berner, 1987) can readily produce Shuram-style carbon isotope excursions. However, our model will only find reasonable solutions when there is a net transfer of oxidizing power from the crust to the ocean-atmosphere system, which we have modeled as a shift in the fraction of sulfur buried as pyrite (f_{py}), although this could in principle also be tied to a shift in the Fe cycle (e.g., an imbalance in the ferric/ferrous ratio of iron being weathering versus iron being buried).

In any case, the preponderance of data suggests that the minimum magnitude of our invoked S cycle shift is reasonable. For instance, the magnitude of our invoked shift in f_{py} is less than that proposed during short- and long-term perturbations to the global sulfur cycle during the Phanerozoic (Canfield & Farquhar, 2009; Hurtgen

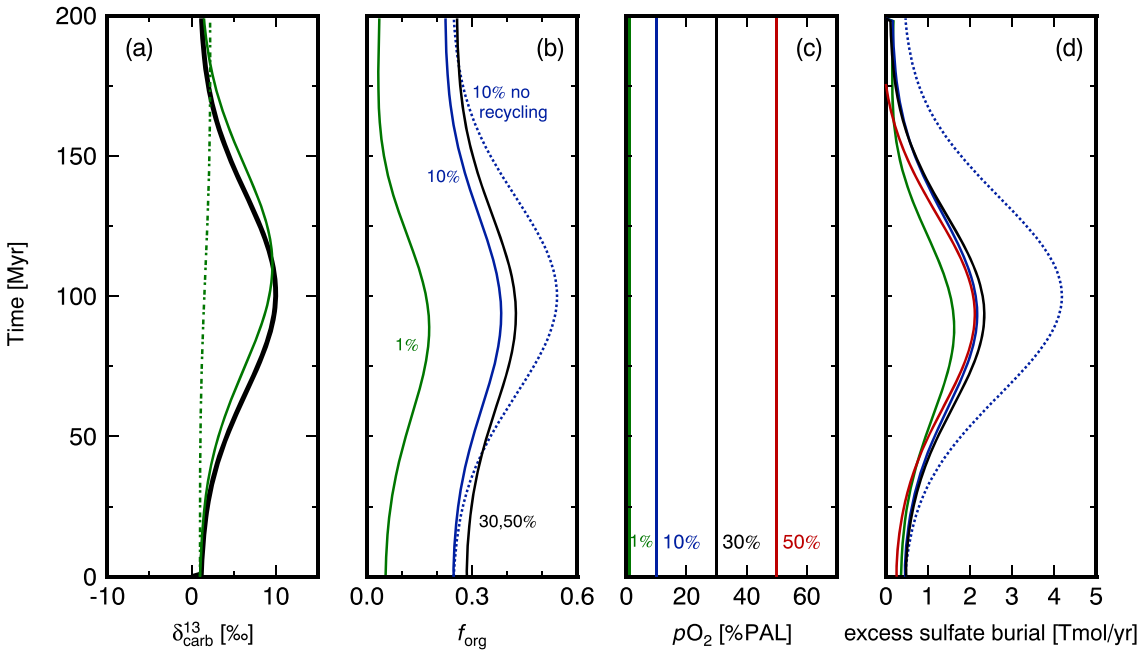

Figure 4. (a) The idealized evolution of the isotopic value of marine DIC during the Lomagundi excursion (black). The green lines show the isotopic value of the young (dotted) and old (dashed) carbonate crustal reservoirs. (b) Modeled changes to the relative organic carbon burial flux (f_{org}). Models assuming static atmospheric pO_2 of 1% (green), 10% (blue), 30% (black), and 50% PAL (red) are shown. For the 10% case, a run without rapid recycling (dotted blue) is also shown. Here the burial rates of 30% and 50% overlap with each other. (c) Imposed atmospheric oxygen levels. (d) Modeled evolution of net pyrite consumption (e.g., pyrite oxidation followed by sulfate burial) through the excursion. For the run without rapid recycling, a higher organic burial rate and a larger redox imbalance is necessary to explain the excursion (dotted blue).

et al., 2002; Gill et al., 2011; Owens et al., 2013; Wu et al., 2010). Our model predicts an increase in surface oxygen levels during the initial stages of the Shuram excursion, which is consistent with recent paleoredox work (carbonate I/Ca ratios) from multiple Shuram archives (Hardisty et al., 2017). This suggests our modeling results are generally consistent with recently emerging geochemical constraints on the Shuram excursion. We have not explicitly modeled the sulfur cycle or sulfur isotope evolution during the Shuram excursion, but comparing our results to recent predictions based on S isotope modeling (Fike et al., 2006; Osburn et al., 2015), it is an obvious topic for future work.

Our model also provides insight into why anomalously light carbon isotope excursions may be limited to the terminal Proterozoic. Our model requires large swings in atmospheric oxygen levels and some transfer of oxidizing potential from the crust to the ocean-atmosphere system (e.g., weathering of evaporites). Evaporite deposition is dependent on having a relatively well-oxygenated ocean-atmosphere system but is also dependent on tectonic and climatic conditions and is thus a pulsed process (e.g., Halevy et al., 2012). The oscillatory nature of sulfate deposition and weathering sets up the potential to transfer oxidants from the crust to the ocean-atmosphere system. However, the Archean and mid-Proterozoic were characterized by low atmospheric oxygen levels and a dearth of massive evaporites. Therefore, this apparently stable Earth system state could not, in our model framework, sustain high-amplitude negative marine $\delta^{13}C_{DIC}$ excursions. In contrast, the Phanerozoic (or at least the Mesozoic and Cenozoic) seems to have been stabilized in a high-oxygen state, potentially mediated by the rise of land plants, and the factors stabilizing a high-oxygen Earth state may have similarly dampened the potential for high-amplitude swings in marine $\delta^{13}C_{DIC}$ values. In addition to changes in weathering efficiency, the burial rate of organic matter may have changed with sea level and the oxygenation of the shallow ocean, which has been proposed to help explain the evolving magnitude and duration of C isotope excursions during Phanerozoic (Bachan et al., 2017). In our model, there are dramatic shifts in the burial rate of organic carbon, but to reproduce the Shuram both rapid recycling of sedimentary organic carbon and oxygen-dependent weathering seem to be additional requirements to replicate the excursion.

4.2. Lomagundi Excursion

If sedimentary recycling and inhibited organic carbon oxidation are not considered, our simplified version of the Lomagundi carbon isotope excursion would cause an extreme release of oxygen. Considering just the C

and S cycles, over 3 Tmol/year sulfate burial (from weathered pyrites) would be needed to maintain a pO_2 of 100% PAL. This sulfate burial flux is larger than the modern total sulfur input term. Although it has been proposed that the Archean crust may have been more S-rich than the modern continental crust (Bekker et al., 2004), this scenario seems unlikely, given the likelihood of pyrite subduction under an anoxic ocean (Canfield, 2004; Reinhard et al., 2013) and the unlikelihood of all S burial from the ocean as sulfate. Even in the well-oxygenated Cenozoic oceans, the maximum sulfate burial fluxes are thought to be only 50% of the input flux (Berner & Berner, 2012). It is possible that there was also a shift in the burial ratio of reduced to oxidized iron (e.g., Bachan & Kump, 2015). However, there is no strong evidence for such a shift and extensive iron oxide burial may have occurred even in the oxygen-poor oceans of the Archean (e.g., Konhauser et al., 2017). Regardless, inclusion of sedimentary recycling dramatically reduces the modeled total oxidant flux. If atmospheric oxygen levels were relatively low—such that organic matter oxidation was inhibited—the modeled total oxidant flux decreases even further. Some Lomagundi model simulations may be implausible, given that in spite of low pO_2 levels, significant marine sulfate burial occurs (e.g., Figure 4). However, the small redox imbalance modeled here as a crustal S redox shift (e.g., 1 Tmol/year) could also be accounted for by enhanced hydrothermal or volcanogenic reductant fluxes (e.g., Laakso & Schrag, 2017).

5. Conclusions

We have demonstrated that including sedimentary recycling and an oxygen dependence on organic carbon oxidation in global carbon cycle models dramatically reduces the magnitude of the carbon cycle perturbations needed to drive anomalously negative or positive marine $\delta^{13}C_{DIC}$ values. Although both of these processes have been utilized in a number of biogeochemical models (Berner, 1987; Daines et al., 2017; Reinhard et al., 2013), they have not been explored with respect to the two largest putative global carbon isotope excursions in Earth's history—the Lomagundi and Shuram carbon isotope excursions. Collectively, these processes alleviate the oxidant paradoxes raised by the magnitude of these excursions. In particular, it possible to have a massive negative carbon isotope excursion—such as the Shuram excursion—without an oxidant shortage so long as atmospheric oxygen levels are allowed to vary substantially. Further, considering sedimentary recycling of heavy carbon back into the weatherable shell, it is possible to have massive, long-lived positive carbon isotope excursion without requiring unrealistically large organic carbon burial fluxes or transiting to a well-oxygenated Earth state.

Appendix A: Model Description

Equations (1)–(6) describe the key part of our model, but a few additional equations are necessary to solve the model. Table A1 shows the values or the formulation of each parameter. In section 2, we emphasized that the weathering flux of organic carbon changes as a function of pO_2, but a number of other fluxes are allowed to evolve dynamically. One of those is the total burial flux. The total burial flux is modified according to the input flux to the surface, which includes organic carbon weathering $F_{w,org}$ and is partitioned between carbonate and organic carbon using a f_{org} calculated to match a given marine $\delta^{13}C$ value. In order to maintain a constant size for each carbon reservoir, a fraction of the burial is assumed to return to the mantle. This yields the following expressions for the evolution of young crustal reservoirs:

$$\frac{dM_{carb,y}}{dt} = F^{b,carb}_{surf\rightarrow y} - F_{carb,y\rightarrow surf} - F_{carb,y\rightarrow o} = 0 \quad (A1)$$

and

$$\frac{dM_{org,y}}{dt} = F^{b,org}_{surf\rightarrow y} - F_{org,y\rightarrow surf} - F_{org,y\rightarrow o} = 0, \quad (A2)$$

where the parameters are defined in Table A1. Ignoring the return flux of carbon to the mantle has a negligible effect on our results. The additional carbon from the mantle is substantially smaller than the size of the crustal reservoirs, and it will only be 1% of the overall surface reservoir size even after a period of 10–30 Myr.

For completeness, the evolution of young and old organic carbon reservoirs is given as follows:

$$\frac{d\delta_{org,y}}{dt} = \frac{F^{b,org}_{surf\rightarrow y}(\delta_{carb} + \Delta_B - \delta_{org,y})}{M_{org,y}}, \quad (A3)$$

Table A1
Model Parameters and Values Used in the Model

Parameter	Description	Model value
M_0	Atmospheric and oceanic carbon mass	3,900 Tmol
$M_{carb,y}$	Mass of young (rapidly weathering) carbonate reservoir	4.0×10^8 Tmol
$M_{carb,o}$	Mass of old (slowly weathering) carbonate reservoir	4.0×10^9 Tmol
$M_{org,y}$	Mass of young (rapidly weathering) organic carbon reservoir	1.0×10^8 Tmol
$M_{org,o}$	Mass of old (slowly weathering) organic carbon reservoir	1.0×10^9 Tmol
f_{org}	Relative fraction of organic carbon to the total burial flux	Solved
$F_{b,carb}$	Burial flux of carbonate	$(1 - f_{org})F_w$
$F_{b,org}$	Burial flux of organic carbon	$f_{org}F_w$
$F^{b,carb}_{surf\rightarrow y}$	Carbonate burial flux added to young carbonate crustal reservoir	34,000 Tmo/kyr
$F^{b,org}_{surf\rightarrow y}$	Organic carbon burial flux added to young organic carbon reservoir	$F_{w,org}$
F_w	Total weathering flux ($= F_{w,carb} + F_{w,org} + F_{volc} + F_{CH_4}$)	Solved
$F_{w,carb}$	Total carbonate weathering flux ($= F_{carb,y\rightarrow surf} + F_{carb,o\rightarrow surf}$)	Solved
$F_{w,org}$	Total organic carbon weathering flux ($= F_{org,y\rightarrow surf} + F_{org,o\rightarrow surf}$)	From supporting information Figure S3
$F_{carb,y\rightarrow surf}$	Weathering flux of carbonate from young crustal reservoir	27,200 Tmol/kyr
$F_{carb,o\rightarrow surf}$	Weathering flux of carbonate from old crustal reservoir	6,800 Tmol/kyr
$F_{carb,y\rightarrow o}$	Transporting flux of carbonate from young to old crustal reservoir	6,800 Tmol/kyr
$F_{org,y\rightarrow surf}$	Weathering flux of organic carbon from young crustal reservoir	$0.8F_{w,org}$
$F_{org,o\rightarrow surf}$	Weathering flux of organic carbon from old crustal reservoir	$0.2F_{w,org}$
$F_{org,y\rightarrow o}$	Transporting flux of organic carbon from young to old crustal reservoir	$0.2F_{w,org}$
F_{volc}	Volcanic carbon flux	6,000 Tmol/kyr
F_{CH_4}	Methane flux	1,000 Tmol/kyr
$\delta_{w,carb}$	Isotopic value of carbonate weathering flux	Solved by equation (5)
$\delta_{carb,y}$	Isotopic value of young carbonate crustal reservoir (−1‰ for initial)	Solved by equation (3)
$\delta_{carb,o}$	Isotopic value of old carbonate crustal reservoir (−1‰ for initial)	Solved by equation (4)
$\delta_{w,org}$	Isotopic value of carbonate weathering flux	Solved by equation (A5)
$\delta_{org,y}$	Isotopic value of young organic carbon reservoir (−31‰ for initial)	Solved by equation (A3)
$\delta_{org,o}$	Isotopic value of old organic carbon reservoir (−31‰ for initial)	Solved by equation (A4)
δ_{volc}	Isotopic value of volcanic carbon flux	−5.5‰
δ_{CH_4}	Isotopic value of methane flux	−60‰

$$\frac{d\delta_{org,o}}{dt} = \frac{F_{org,y\rightarrow o}(\delta_{org,y} - \delta_{org,o})}{M_{org,o}}, \tag{A4}$$

and

$$\delta_{w,org} = \frac{F_{org,y\rightarrow surf}\delta_{org,y} + F_{org,o\rightarrow surf}F_{org,o\rightarrow surf}}{F_{org,y\rightarrow surf} + F_{org,o\rightarrow surf}}, \tag{A5}$$

where the description of each parameter is again given in Table A1. All ordinary differential equations are solved using forward finite difference discretization.

Acknowledgments
The carbon isotope data for Shuram excursion are taken from Fike et al., (2006; doi: 10.1038/nature05345). N. J. P., E. W. B., and C. T. R. were funded through the Alternative Earths NASA Astrobiology Institute and E. W. B. received support from Virtual Planetary Laboratory NASA Astrobiology Institute. This work was supported in part by the facilities and staff of the Yale University Faculty of Arts and Sciences. We are grateful to Maggie Osburn and Lee Kump for constructive comments.

References

Bachan, A., & Kump, L. R. (2015). The rise of oxygen and siderite oxidation during the Lomagundi Event. *Proceedings of the National Academy of Sciences*, *112*(21), 6562–6567. https://doi.org/10.1073/pnas.1422319112

Bachan, A., Lau, K. V., Saltzman, M. R., Thomas, E., Kump, L. R., & Payne, J. L. (2017). A model for the decrease in amplitude of carbon isotope excursions across the Phanerozoic. *American Journal of Science*, *317*, 641–676. https://doi.org/10.2475/06.2017.01

Bartley, J. K., & Kah, L. C. (2004). Marine carbon reservoir, Corg-Ccarb coupling, and the evolution of the Proterozoic carbon cycle. *Geology*, *32*(2), 129–132. https://doi.org/10.1130/G19939.1

Bekker, A. (2014). Lomagundi carbon isotope excursion andrey. In G. Gargaud (Ed.), *Encyclopedia of astrobiology* (pp. 1–6) . Berlin: Springer. https://doi.org/10.1007/978-3-662-44185-5

Bekker, A., & Holland, H. D. (2012). Oxygen overshoot and recovery during the early Paleoproterozoic. *Earth and Planetary Science Letters*, *317-318*, 295–304. https://doi.org/10.1016/j.epsl.2011.12.012

Bekker, A., Holland, H. D., Wang, P. L., Rumble, D. I., Stein, H. J., Hannah, J. L., et al. (2004). Dating the rise of atmospheric oxygen. *Nature*, *427*, 117–120. https://doi.org/10.1038/nature02260

Bekker, A., Planavsky, N. J., Krapez, B., Rasmussen, B., Hoffman, A., Slack, J. F., et al. (2014). Iron formations: Their origins and implications for ancient seawater chemistry. In H. D. Holland & K. Turekian (Eds.), *Treatise on geochemistry* (Vol. 9, pp. 561–628). New York: Elsevier. https://doi.org/10.1016/B978-0-08-095975-7.00719-1

Berner, R. A. (1987). Models for carbon and sulfer cycles and atmospheric oxygen: Application to Paleozoic gelogic history. *American Journal of Science*, *287*, 177–196.

Berner, E. K., & Berner, R. A. (2012). *Global environment water, air, and geochemical cycles* (488 pp.)., Princeton, NJ: Princeton University Press.

Bjerrum, C. J., & Canfield, D. E. (2011). Towards a quantitative understanding of the late Neoproterozoic carbon cycle. *Proceedings of the National Academy of Sciences*, *108*(14), 5542–5547. https://doi.org/10.1073/pnas.1101755108

Blättler, C. L., Claire, M. W., Prave, A. R., Kirsimäe, K., Higgins, J. A., Medvedev, P. V., et al. (2018). Two-billion-year-old evaporites capture Earth's great oxidation. *Science*, *360*, 320–323. https://doi.org/10.1126/science.aar2687

Bolton, E. W., Berner, R. A., & Petsch, S. T. (2006). The weathering of sedimentary organic matter as a control on atmospheric O_2: II. Theoretical modeling. *American Journal of Science*, *306*, 575–615. https://doi.org/10.2475/08.2006.01

Bristow, T. F., & Kennedy, M. J. (2008). Carbon isotope excursions and the oxidant budget of the Ediacaran atmosphere and ocean. *Geology*, *36*(11), 863–866. htttps://doi.org/10.1130/G24968A.1

Bristow, T. F., Kennedy, M. J., Morrison, K. D., & Mrofka, D. D. (2012). The influence of authigenic clay formation on the mineralogy and stable isotopic record of lacustrine carbonates. *Geochimica et Cosmochimica Acta*, *90*, 64–82. https://doi.org/10.1016/j.gca.2012.05.006

Brocks, J. J., Jarrett, A. J., Sirantoine, E., Hallmann, C., Hoshino, Y., & Liyanage, T. (2017). The rise of algae in Cryogenian oceans and the emergence of animals. *Nature*, *548*(7669), 578–581. https://doi.org/10.1038/nature23457

Burns, S. J., & Matter, A. (1993). Carbon isotopic record of the latest Proterozoic from Oman. *Eclogae Geologicae Helvetiae*, *86*, 595–607.

Calver, C. R (2000). Isotope stratigraphy of the Ediacarian (Neoproterozoic III) of the Adelaide Rift Complex, Australia, and the overprint of water column stratification. *Precambrian Research*, *100*, 121–150. https://doi.org/10.1016/S0301-9268(99)00072-8

Canfield, D. E (1998). A new model for Proterozoic ocean chemistry. *Nature*, *396*, 450–453. https://doi.org/10.1038/24839

Canfield, D. E. (2004). The evolution of the Earth surface sulfur reservoir. *American Journal of Science*, *304*, 839–861.

Canfield, D. E., & Farquhar, J. (2009). Animal evolution, bioturbation, and the sulfate concentration of the oceans. *Proceedings of the National Academy of Sciences of the United States of America*, *106*(20), 8123–8127. https://doi.org/10.1073/pnas.0902037106

Cole, D. B., Reinhard, C. T., Wang, X., Gueguen, B., Halverson, G. P., Gibson, T., et al. (2016). A shale-hosted cr isotope record of low atmospheric oxygen during the Proterozoic. *The Geological Society of America*, *44*(7), 555–558. https://doi.org/10.1130/G37787.1

Daines, S. J., Mills, B. J., & Lenton, T. M. (2017). Atmospheric oxygen regulation at low Proterozoic levels by incomplete oxidative weathering of sedimentary organic carbon. *Nature Communications*, *8*(14), 379. https://doi.org/10.1038/ncomms14379

Derry, L. A. (2010). A burial diagenesis origin for the Ediacaran Shuram-Wonoka carbon isotope anomaly. *Earth and Planetary Science Letters*, *294*, 152–162. https://doi.org/10.1016/j.epsl.2010.03.022

Derry, L. A. (2015). Causes and consequences of mid-Proterozoic anoxia. *Geophysical Research Letters*, *42*, 8538–8546. https://doi.org/10.1002/2015GL065333

Fike, D. A., Grotzinger, J. P., Pratt, L. M., & Summons, R. E. (2006). Oxidation of the Ediacaran ocean. *Nature*, *444*(7120), 744–747. https://doi.org/10.1038/nature05345

Gill, B. C., Lyons, T. W., & Jenkyns, H. C. (2011). A global perturbation to the sulfur cycle during the Toarcian Oceanic Anoxic Event. *Earth and Planetary Science Letters*, *312*, 484–496. https://doi.org/10.1016/j.epsl.2011.10.030

Gong, Z., Kodama, K. P., & Li, Y. X. (2017). Rock magnetic cyclostratigraphy of the Doushantuo Formation, South China and its implications for the duration of the Shuram carbon isotope excursion. *Precambrian Research*, *289*, 62–74. https://doi.org/10.1016/j.precamres.2016.12.002

Halevy, I., Peters, S. E., & Fischer, W. W. (2012). Sulfate burial constraints on the Phanerozoic sulfur cycle. *Science*, *337*, 331–334. https://doi.org/10.1126/science.1220224

Halverson, G. P., Hoffman, P. F., Schrag, D. P., Maloof, A. C., & Rice, A. H. N. (2005). Toward a Neoproterozoic composite carbon-isotope record. *Geological Society of America Bulletin*, *117*(9), 1181. https://doi.org/10.1130/B25630.1

Hardisty, D. S., Zhou, X., Diamond, C. W., & Lyons, T. W. (2017). Perspectives on Proterozoic surface ocean redox from iodine contents in ancient and recent carbonate. *Earth and Planetary Science Letters*, *463*, 159–170. https://doi.org/10.1016/j.epsl.2017.01.032

Hayes, J. M., Kaufman, A., & Strauss, H. (1999). The abundance of ^{13}C in marine organic matter and isotopic fractionation in the global biogeochemical cycles of carbon during the past 800 Ma. *Chemical Geology*, *161*, 103–125.

Holland, H. D. (1984). *The chemical evolution of the atmosphere and oceans* (598 pp.). Princeton, NJ: Princeton University Press.

Holland, H. D. (2002). Volcanic gases, black smokers, and the great oxidation event. *Geochimica et Cosmochimica Acta*, *66*(21), 3811–3826. https://doi.org/10.1016/S0016-7037(02)00950-X

Hurtgen, M. T., Arthur, M. A., Suits, N. S., & Kaufman, A. J. (2002). The sulfur isotopic composition of Neoproterozoic seawater sulfate: Implications for a snowball Earth?

Karhu, J. A., & Holland, H. D. (1996). Carbon isotopes and the rise of atmospheric oxygen. *Geology*, *24*(10), 867–870. https://doi.org/10.1130/0091-7613(1996)024<0867:CIATRO>2.3.CO

Knauth, L. P., & Kennedy, M. J. (2009). The late Precambrian greening of the Earth. *Nature*, *460*, 728–732. https://doi.org/10.1038/nature08213

Knoll, A. H. (2015). Paleobiological perspectives on early microbial evolution. *Cold Spring Harbor Perspectives in Biology*, *6*, a018093. https://doi.org/10.1101/cshperspect.a018093

Konhauser, K. O., Planavsky, N. J., Hardisty, D. S., Robbins, T. J., Warchola, T. J., Haugaard, R., et al. (2017). Iron formations: A global record of neoarchaean to Palaeoproterozoic environmental history. *Earth-Science Reviews*, *172*, 140–177. https://doi.org/10.1016/j.earscirev.2017.06.012

Krissansen-Totton, J., Buick, R., & Catling, D. C. (2015). A statistical analysis of the carbon isotope record from the Archean to Phanerozoic and implications for the rise of oxygen. *American Journal of Science*, *315*, 275–316. https://doi.org/10.2475/04.2015.01

Kump, L. R. (2008). The rise of atmospheric oxygen. *Nature*, *451*, 277–278. https://doi.org/10.1038/nature06587

Kump, L. R., & Arthur, M. A. (1999). Interpreting carbon-isotope excursions: Carbonates and organic matter. *Chemical Geology*, *161*, 181–198. https://doi.org/10.1016/S0009-2541(99)00086-8

Kump, L. R., Junium, C., Arthur, M. A., Brasier, A., Fallick, A. E., & Luo, G. (2011). Isotopic evidence for massive oxidation of organic matter following the great oxidation event. *Science*, *334*, 1694–1696.

Lécuyer, C., & Ricard, Y. (1999). Long-term fluxes and budget of ferric iron: Implication for the redox states of the Earth's mantle and atmosphere. *Earth and Planetary Science Letters*, *165*, 197–211. https://doi.org/10.1016/S0012-821X(98)00267-2

Laakso, T. A., & Schrag, D. P. (2017). *Geobiology*, *15*, 366–384. https://doi.org/10.1111/gbi.12230

Le Guerroue, E., Allen, P. A., Cozzi, A., Etienne, J. L., & Fanning, M. (2006). 50 Myr recovery from the largest negative $\delta^{13}C$ excursion in the Ediacaran ocean. *Terra Nova*, *18*, 147–153. https://doi.org/10.1111/j.1365-3121.2006.00674.x

Lee, C., Fike, D. A., Love, G. D., Sessions, A. L., Grotzinger, J. P., Summons, R. E., & Fischer, W. W. (2013). Carbon isotopes and lipid biomarkers from organic-rich facies of the Shuram Formation, Sultanate of Oman. *Geobiology*, *11*(5). https://doi.org/10.1111/gbi.12045

Lindsay, J. F., & Brasier, M. D. (2002). Did global tectonics drive early biosphere evolution? Carbon isotope record from 2.6 to 1.9 Ga carbonates of western Australian basins. *Precambrian Research*, *114*, 1–34. https://doi.org/10.1016/S0301-9268(01)00219-4

Liu, X. M., Kah, L., Knoll, A., Cui, H., Kaufman, A., Shahar, A., & Hazen, R. (2016). Tracing Earth's O_2 evolution using Zn/Fe ratios in marine carbonates. *Geochemical Perspectives Letters*, *2*, 24–34. https://doi.org/10.7185/geochemlet.1603

Lyons, T. W., Reinhard, C. T., & Planavsky, N. J. (2014). The rise of oxygen in Earth's early ocean and atmosphere. *Nature*, *506*(7488), 307–315. https://doi.org/10.1038/nature13068

McFadden, K. a., Huang, J., Chu, X., Jiang, G., Kaufman, A. J., Zhou, C., et al. (2008). *Proceedings of the National Academy of Sciences*, *105*, 3197–3202. https://doi.org/10.1073/pnas.0708336105

Oehlert, A. M., & Swart, P. K. (2014). Interpreting carbonate and organic carbon isotope covariance in the sedimentary record. *Nature Communications*, *5*, 4672. https://doi.org/10.1038/ncomms5672

Osburn, M. R., Owens, J., Bergmann, K. D., Lyons, T. W., & Grotzinger, J. P. (2015). Dynamic changes in sulfate sulfur isotopes preceding the Ediacaran Shuram Excursion. *Geochimica et Cosmochimica Acta*, *170*, 204–224. https://doi.org./10.1016/j.gca.2015.07.039

Owens, J. D., Gill, B. C., Jenkyns, H. C., Bates, S. M., Severmann, S., Kuypers, M. M. M., et al. (2013). Sulfur isotopes track the global extent and dynamics of euxinia during Cretaceous Oceanic Anoxic Event 2. *Proceedings of the National Academy of Sciences*, *110*(46), 18,407–18,412. https://doi.org/10.1073/pnas.1305304110

Partin, C. A., Bekker, A., Planavsky, N. J., Scott, C. T., Gill, B. C., Li, C., et al. (2013). Large-scale fluctuations in Precambrian atmospheric and oceanic oxygen levels from the record of U in shales. *Earth and Planetary Science Letters*, *369-370*, 284–293. https://doi.org/10.1016/j.epsl.2013.03.031

Paulsen, T., Deering, C., Sliwinski, J., Bachmann, O., & Guillong, M. (2017). Evidence for a spike in mantle carbon outgassing during the Ediacaran period. *Nature Geoscience*, *10*, 930–934. https://doi.org/10.1038/s41561-017-0011-6

Planavsky, N. J., Bekker, A., Hofmann, A., Owens, J. D., & Lyons, T. W. (2012). Sulfur record of rising and falling marine oxygen and sulfate levels during the Lomagundi event. *Proceedings of the National Academy of Sciences*, *109*(45), 1–6. https://doi.org/10.1073/pnas.1120387109

Planavsky, N. J., Reinhard, C. T., Wang, X., Thomson, D., Mcgoldrick, P., Rainbird, R. H., et al. (2014). Low mid-Proterozoic atmospheric oxygen levels and the delayed rise of animals. *Science*, *346*, 635–638. https://doi.org/10.1126/science.1258410

Planavsky, N. J., Tarhan, L. G., Bellefroid, E. J., Evans, D. A. D., Reinhard, C. T., Love, G. D., & Lyons, T. W. (2015). Late Proterozoic transitions in climate, oxygen, and tectonics, and the rise of complex life. *The Paleontological Society Papersto*, *21*, 47–82.

Pokrovsky, B., & Gertsev, D. (1993). Upper Precambrian carbonates extremely depleted in ^{13}C. *Lithology and Mineral Resources*, *1*, 64–80.

Reinhard, C. T., Planavsky, N. J., Gill, B. C., Ozaki, K., Robbins, L. J., & Lyons, T. W. (2017). Evolution of the global phosphorus cycle. *Nature*, *541*, 386–389. https://doi.org/10.1038/nature20772

Reinhard, C. T., Planavsky, N. J., & Lyons, T. W. (2013). Long-term sedimentary recycling of rare sulphur isotope anomalies. *Nature*, *497*, 100–103. https://doi.org/10.1038/nature12021

Ridgwell, A., & Schmidt, D. N. (2010). Past constraints on the vulnerability of marine calcifiers to massive carbon dioxide release. *Nature Geoscience*, *3*, 196–200. https://doi.org/10.1038/ngeo755

Rothman, D. H., Hayes, J. M., & Summons, R. E. (2003). Dynamics of the Neoproterozoic carbon cycle. *Proceedings of the National Academy of Sciences*, *100*(14), 8124–8129. https://doi.org/10.1073/pnas.0832439100

Shi, W., Li, C., & Algeo, T. J. (2017). Quantitative model evaluation of organic carbon oxidation hypotheses for the Ediacaran Shuram carbon isotopic excursion. *Science China Earth Sciences*, *60*, 1–10.

Shields, G., & Veizer, J. (2002). Precambrian marine carbonate isotope database: Version 1.1. *Geochemistry, Geophysics, Geosystems*, *3*(6), 1031. https://doi.org/10.1029/2001GC000266

Shields-Zhou, G., & Och, L. (2011). The case for a Neoproterozoic oxygenation event: Geochemical evidence and biological consequences. *GSA Today*, *21*(3), 4–11. https://doi.org/10.1130/GSATG102A.1

Sperling, E. A., Wolock, C. J., Morgan, A. S., Gill, B. C., Kunzmann, M., Halverson, G. P., et al. (2015). Statistical analysis of iron geochemical data suggests limited late Proterozoic oxygenation. *Nature*, *523*, 451–454. https://doi.org./10.1038/nature14589

Thomson, D., Rainbird, R. H., Planavsky, N., Lyons, T. W., & Bekker, A. (2015). Chemostratigraphy of the shaler supergroup, Victoria Island, NW Canada: A record of ocean composition prior to the cryogenian glaciations. *Precambrian Research*, *263*, 232–245. https://doi.org/10.1016/j.precamres.2015.02.007

Turner, E. C., & Bekker, A. (2016). Thick sulfate evaporite accumulations marking a mid-Neoproterozoic oxygenation event (Ten Stone Formation, Northwest Territories, Canada). *Geological Society of America Bulletin*, *128*, 203–222. https://doi.org/10.1130/B31268.1

Wallmann, K., & Aloisi, G. (2012). The global carbon cycle: Geological processes. In A. H. Knoll, et al. (Eds.), *In fundamentals of geobiology* (pp. 20–35). Chichester, UK: Blackwell Publishing Ltd.

Wortmann, U. G., & Paytan, A. (2012). Rapid variability of seawater chemistry. *Science*, *337*, 334–336. https://doi.org/10.1126/science.1220656

Wu, N., Farquhar, J., Strauss, H., Kim, S. T., & Canfield, D. E. (2010). Evaluating the S-isotope fractionation associated with Phanerozoic pyrite burial. *Geochimica et Cosmochimica Acta*, *74*, 2053–2071. https://doi.org/10.1016/j.gca.2009.12.012

Yokota, K., Kanzaki, Y., & Murakami, T. (2013). Weathering model for the quantification of atmospheric oxygen evolution during the Paleoproterozoic. *Geochimica et Cosmochimica Acta*, *117*, 332–347. https://doi.org/10.1016/j.gca.2013.03.015

Zhang, S., Wang, X., Wang, H., Bjerrum, C. J., Hammarlund, E. U., Costa, M. M., et al. (2016). Sufficient oxygen for animal respiration 1,400 million years ago. *Proceedings of the National Academy of Sciences*, *113*(7), 1731–1736. https://doi.org/10.1073/pnas.1523449113